*First International Conference on Scour of Foundations, ICSF-1*
*Texas A&M University, College Station, Texas, USA November 17-20, 2002*

# Pier and Abutment Scour-New Laboratory Data

by

Willi H. Hager[1], Jens Unger[2] ,Giuseppe Oliveto[3]

## ABSTRACT

The purpose of this paper is threefold: (1) Presentation of a scour installation used over the past 6 years, (2) Summary of results pertaining to the Shields entrainment criterion that was expanded for bridge pier and bridge abutment; and (3) Discussion of new results. Based on a long term investigation of scour, the experimental method was improved to result presently in an installation that might be of general interest. Accordingly, details of the set-up are highlighted that allowed the analysis of both the entrainment criterion and the temporal development of bridge scour. Based on a wide range of pier and abutment geometries, various uniform and non-uniform sediments, and densimetric particle Froude numbers up to the threshold condition, both a generalized Shields formulation, and an equation for temporal scour progress were derived. These results are readily applicable for design, given the selection of basic parameters in the novel approach. They are highlighted with an example that illustrates also the accuracy of the present approach.

KEY WORDS: Abutment scour, Bridge hydraulics, Inception of transport, Movable bed, Pier scour, Scour inception, Shields'criterion.

## INTRODUCTION

Scour has received significant attention in the past decades (Raudkivi 1998). Until recently, engineers employed scour equations that would mainly give some indication on the so-called end scour depth. Due to various difficulties in observing scour progress it was proposed that something like an end scour occurs after 2, maybe 6 or even more hours, mainly because observations could not be continued because of the progressively poorer hydraulic conditions in the scour channel. A comparison with prototype scour demonstrated at once significant differences with those scour equations, and research started to care for temporal scour development as one of the significant effects. Recently, the present authors presented a novel scour equation that satisfies the similarity criterion according to Froude. Using a large data basis collected at Versuchsanstalt für Wasserbau, Hydrologie und Glaziologie VAW, ETH Zurich, a scour equation was presented to demonstrate the significant effect of the densimetric Froude number. A time scale was derived using also the Froude law. The equation proposed and also presented in this paper was verified with all existing laboratory data accessible to the authors (Oliveto and Hager 2002), and a reasonable agreement was observed.

The purposes of the present paper are: (1) Presenting the VAW scour installation and procedure for obtaining long-time scour series, (2) Review of previous results relative to a generalized entrainment condition for scour inception, that simplifies to the Shields approach for a pier of infinitesimally small diameter. Also, the relation for temporal scour progress is reviewed, and (3) Application of the present results to an example to compare the present predictions.

[1] Professor, VAW, ETH-Zentrum, CH-8092 Zurich, Switzerland, (hager@vaw.baug.ethz.ch)
[2] Research student, VAW, ETH-Zentrum, CH-8092 Zurich, Switzerland, (unger@vaw.baug.ethz.ch)
[3] Dr., DIFA, Università della Basilicata, I-85100 Potenza, Italy, (oliveto@unibas.it)

## EXPERIMENTS

*Experimental Setup*

VAW initiated scour research in 1995 by focusing so-called building scour. The scour channel set up satisfied special demands in this field of hydraulics. The experiments were conducted in a rectangular channel of width $B$ = 1.00 m, depth of 0.70 m to the sediment surface, and length of 13 m, with a working section of about 5 m (Fig.1). The sediment surface was always inserted horizontal because of the *local* scour phenomenon. The channel was finished in smoothened steel, except for the left channel side made of a 43 mm thick glass wall to allow for observation. A pump with a maximum discharge capacity of 130 l/s was installed at the upstream channel side and connected to a stainless steel pipe with an internal diameter of 250 mm. A flow straightener made of geotextile mattresses was inserted at the transition between rigid and loose bed upstream of the test reach. Its purposes were: (1) Horizontal upstream water surface, (2) Elimination of macro-vortices due to asymmetric water supply, (3) Uniform velocity and discharge distributions in the upstream test reach, (4) Flow free of surface waves, (5) Elimination of macro-turbulence in loose bed intake reach originating from the sides of the intake, and (6) Overall excellent flow appearance to generate long-time scour observations (Fig.1a).

A fully submerged weir type structure at the downstream end of the test reach avoids sediment transport out of the scour area. A flap gate allowed external control of the water surface elevation to the nearest millimeter (Fig. 1b). A vertical filter wall prevented air bubbles to enter the return pipe. Further details are described by Hager et al. (2002). The present VAW installation allows to conduct scour tests of easily 1 week, with periods of up to 12 weeks having also been investigated.

*Instrumentation*

Piers and abutments were fabricated of plexiglass to the next millimeter to enable visual observation across these elements. Light sheets were mounted into a pier or an abutment, to study the velocity field. Piers of diameters $D$ = 0.022, 0.050, 0.064, 0.110, 0.257, 0.400, and 0.500 m were used, and abutments had widths $b$ = 0.05, 0.10, 0.20, 0.40, and 0.60 m measured from the channel side towards the channel axis. Maximum setting accuracy of an element was 1 to 2 mm.

Scour experiments were directed to observe both sediment and water surfaces. These characteristics were determined with conventional gauges. Axial and transverse water surface profiles were taken, in addition to particular points such as the stagnation flow depth upstream of the elements. The reading accuracy was within 1 mm, except for locations with a pronounced surface turbulence or standing surface waves. The sediment surface was observed with a shoe gauge, given its similarity with a shoe of 5 mm length to 2 mm width. Sediment surface readings were then much simpler than with a conventional point gauge with an accuracy of about 0.5 sediment diameter, or 1 mm.

Sediment readings involved the original bed elevation, the upstream beginning of scour, the transverse extent of scour at the element upstream and downstream sides, the maximum scour depths at these two locations, the location of maximum aggradation downstream of the elements besides particular points for each test. Test readings were made in short intervals close to the beginning, and at longer intervals after the initial scour phase. Normally, the main observations were conducted at 1, 3, 6, 10, and 20 minutes from scour initiation, and then followed in hours, half days, 1 day, and so on until additional readings were considered no more interesting.

Three sediments of almost uniform average size of 0.55, 3.3 and 4.8 mm, and three mixtures, with $d_{50}$ = 5.3, 1.2, 3.1 mm, and $\sigma = (d_{84}/d_{16})^{1/2}$ = 1.43, 1.80 and 2.15, respectively, were used. These sediments allowed to specify the effects of average grain size and sediment non-uniformity on scour initiation and scour progress. An additional plastic sediment with a density $\rho_s$ = 1.42 t/m$^3$ was employed to check for the density effect.

*Experimental procedure*

To obtain a horizontal sediment surface for scour initiation, a grading mechanism was employed, resembling a snow plough with a rectangular vertical plate at its downstream side. Sediment grading was always made under water of several centimeters height, because of ease in sediment movement (Hager et al. 2002).

To initiate an experiment, the flap gate was lifted to a position that would submerge the working section beyond sediment entrainment. The pump was started and discharge increased to the selected value, thereby carefully inhibiting sediment movement especially around the sides of the pier. Using the flap gate, the water surface elevation was carefully lowered, until inception of sediment transport around the element started. Once first particles moved (Hager and Oliveto 2002), the time origin was set to zero, and the water surface lowered to test conditions. Surface drawdown was completed within some seconds, to allow for the first reading of the sediment surface after 1 minute. In total almost 400 experiments were completed within the past 3 years, with a typical experimental duration of 2.5 days. The effects of upstream velocity, sediment size, sediment density, flow depth, pier diameter and abutment width were investigated resulting in two main papers. The first paper relates to the extended Shields entrainment criterion with piers or abutments present in a loose boundary flow, whereas the second predicts pier and abutment scour depth as a function of time, by accounting for all of the previously mentioned parameters (Hager and Oliveto 2002, Oliveto and Hager, 2002). In the following some observations during scour progress will be described.

*Scour Initiation*

Scour initiated once the upstream velocity $V_o = Q/Bh_o$ was equal to the entrainment (inception subscript $i$) velocity $V_i$ with $Q$ as discharge, $B$ channel width and $h_o$ upstream flow depth. In a flow without any elements the entrainment criterion for the viscous ($D_* \le 10$), the transition ($10 < D_* < 150$) and the fully rough turbulent ($D_* \ge 150$) regimes, where $D_* = (g'/\nu^2)^{1/3} d_{50}$ with $g' = [(\rho_s - \rho)/\rho]g$ as the relative gravitational acceleration and $\nu$ as kinematic viscosity is (Hager and Oliveto 2002)

$$F_{di} = 2.33 D_*^{-0.25} \left(R_h / d_{50}\right)^{1/6}, \qquad D_* \le 10 \tag{1}$$

$$F_{di} = 1.08 D_*^{1/12} \left(R_h / d_{50}\right)^{1/6}, \qquad 10 < D_* < 150 \tag{2}$$

$$F_{di} = 1.65 \left(R_h / d_{50}\right)^{1/6}, \qquad D_* < 150 \tag{3}$$

Here, $F_{di} = V_i/(g' d_{50})^{1/2}$ is the densimetric particle inception Froude number, $R_h$=hydraulic radius and $d_{50}$ = average grain size. For the first two cases, $F_{di}$ is proportional to a power of dimensionless grain size $D_*$, and increases with the relative hydraulic radius. For constant densities of sediment and fluid, the inception Froude number thus increases with the relative flow depth.

For a plane sediment bed containing a pier an additional effect may thus be observed that tends to zero for an extremely small pier diameter $D$. All effects originating from fluid flow and sedimentology are confined in (1) to (3), and the addition of relative pier diameter causes a purely geometrical effect. The effect of pier contraction $\beta = D/B < 0.65$ may be accounted for by the ratio $\Phi_\beta = F_d/F_{di}$ between the cases when the pier is present $F_d$, and the pier is absent as (Hager and Oliveto 2002)

$$\Phi_\beta = 1 - 1.10 (2/3) \beta^{1/4} \tag{4}$$

Accordingly, sediment entrainment results in larger velocities for small relative pier diameters, and smaller velocities for large piers. Equation (4) states that no sediment transport occurs for a velocity $V_o$ smaller than the entrainment velocity $V_i$ of a pier. This lower limit of sediment entrainment has so far not been specified.

*Scour progress*

Most of the observations currently available refer exclusively to the scour depth, while other details of scour progress remain obscure. For pier scour, scour initiation is always at the upstream lateral side of the cylinder, roughly at 70° when 0 is the upstream axial direction from the center of pier. Depending on $F_d$, one may refer to small, medium or fast scour progress. For $F_{di} < F_d < 2$, scour is weak with a tendency for slightly asymmetric scour on the two pier sides. Typical clear water scour may be expected for $2 < F_d < F_{dt}$, with a significant effect of pier diameter on the scour extension. For $F_d > F_{dt}$, i.e. over the threshold (subscript *t*) condition of the upstream bed, scour does not really advance after a sufficient time because of an equilibrium between sediment transports into and out of the scour hole (Graf and Altinakar 1997, Hoffmans and Verheij 1997). This latter regime was not investigated in the present work because inaccuracies complicate data analysis.

Scour progress in the typical domain of densimetric particle Froude numbers between 2 and 3 can be described as follows (Fig. 2). Scour initiates at the sides of the cylinder, at an angle of approximately 70°, where the bottom shear stresses are expected to be a maximum due to acceleration of flow across the contraction by the pier. Material is washed downstream into the zone where velocity decreases, and thus aggradation starts at the end of the cylinder, close to the shear layer between the forward main flow and the recirculating wake flow of the cylinder. Progress of scour at the first stage is very strong, both in terms of scour and aggradation heights. Note that there is absolutely no scour at the upstream side of the cylinder, because of stagnation flow.

Figure 3 relates to lateral observation of scour progress, in which again scour initiation may be observed slightly upstream from the pier axis, then advancing to the upstream pier side at phase 3. Simultaneously, the aggradation of sediment reaches a maximum at about that stage, and then progressively is shifted downstream from the cylinder. It can also be seen that the scour maximum stays on the side of the pier until phase 5 and then migrates upstream to the leading face of the pier. This temporal progress of scour is typical for piers (and also abutments), with a maximum scour depth at the upstream face only at an advanced scour stage. An exception may occur for flow conditions with a densimetric Froude number very close to the entrainment condition. Then, this shift of scour maximum from the pier side to upstream of the pier does not occur because of too small forces involved after the initial scour phase.

At the end of the first stage, scour surface has extended both against and in the flow direction, with the scour maximum shifted upstream towards the pier axis. The second scour stage then starts. Most of the past descriptions of pier scour did not specify the migration of scour maximum against flow direction, and measurements were confined exclusively to the growth in the pier axis. Oliveto and Hager (2002) proposed an equation for scour progress both for pier and abutment. These two geometries differ only by a shape factor equal to $N$=1 for the pier, and $N$=1.25 for the abutment. For otherwise identical conditions, abutment scour is thus by 25% larger than pier scour.

The relative pier scour depth $Z = z/(D^{2/3}h_o^{1/3})$ depends essentially on: (1) Densimetric Froude number $F_d = (\sigma^{-1/3}V_o)/(g'd_{50})^{1/2}$ where $\sigma = (d_{84}/d_{16})^{1/2}$ is the standard deviation of sediment mixture, equal to 1 for a uniform sediment, and (2) Time scale $T = [\sigma^{1/3}(g'd_{50})^{1/2}/D^{2/3}h_o^{1/3}]t$ with $t$ as time relative to scour initiation, as previously mentioned. The relation

$$Z = 0.068\, N\, F_d^{1.5} \log(T), \qquad F_{di} < F_d < F_{dt} \tag{5}$$

was established with the VAW data set and verified with the available literature data. In total some 600 scour progress series were employed to establish (5), resulting in a maximum standard deviation of some 10%. Details for the application of (5) were also provided by Oliveto and Hager (2002).To check the previous approach with a typical experiment, consider the following problem: $Q$ = 0.107 l/s, $h_o$ = 0.197 m, $V_o$ = 0.54 m/s, $D$ = 0.257 m, g' = 16.19 m/s$^2$, $d_{50}$ = 0.0055 mm, $\sigma$ = 2.26, thus $F_d$ =1.38. The non-dimensional time $T$ can be expressed as $T = t/t_R$ with the reference time $t_R = [\sigma^{1/3}(g'd_{50})^{1/2}/D^{2/3}h_o^{1/3}]^{-1}$ = 0.60 s. Figure 4 compares that particular experiment with the prediction according to (5), and a reasonable agreement between the two is noted.

## VELOCITY DISTRIBUTION

To further knowledge for pier scour, velocity fields around a pier were observed, with a typical case being presented below. The test conditions were as for the example previously introduced, with a relatively small approach intensity. The velocity distribution was measured with a standard propeller meter to compare results with a more involved experimental technique to be described. The local angles of streamlines relative to the channel axis were measured first with an angle meter and the propeller was then positioned into the previously determined direction. Figure 5 shows plane velocity distributions (a) close to the free surface, (b) at 50% flow depth, (c) close to the original sediment surface, and (d) 50% below that elevation. At the free surface, the velocities may be described as one would expect for a two-dimensional flow around a cylinder. However, at a lower elevation, there appears to be an increase of velocity close to the cylinder, with a forward direction downstream of it. In the scour hole velocities are in about the same direction, yet with an absolute value somewhat smaller as the sediment bed is reached. From present experimental possibilities, such observations are of course crude, but they serve as a calibration for more sophisticated approaches, such as particle image velocimetry PIV or particle tracking. At present, that system is set up, and results will be presented later. Figure 5 (e) is a plot of the water surface with a maximum surface elevation at the stagnation point upstream from the cylinder, and a minimum laterally from the cylinder where scour started. Figure 5 relates to conditions where scour advance is small with a dimensionless time of approximately $T = 10^5$.

## CONCLUSIONS

Bridge hydraulics has become a significant issue in the past years. The present work would like to add to two particular points: (1) Presentation of a hydraulic installation developed at VAW during the past years, with particular attention to the needs of scour investigation, and (2) Extension of Shields entrainment condition with an approach involving basic hydraulic parameters such that it can readily be determined if a pier or an abutment undergoes scour, or not. These results may also be applied to investigate the stability of a natural riverbed. Further, the temporal progress of scour is discussed in terms of a novel proposal taking into account the most significant parameters of pier scour. This relation resulted from extensive model observations and was tested with the available literature scour tests. As a third point, details of scour advance are described in terms of photographs taken from various locations. It is clearly stated that the maximum scour depth occurs only at an advanced stage upstream from the pier. Velocity distributions taken with a propeller may be used for calibration purposes but do not allow sufficient insight into the complex flow field around a pier. The need for advanced experimental instrumentation is outlined.

## REFERENCES


1. Graf, W.H., Altinakar, M.S. (1996) *Hydraulique fluviale*. Presses Polytechniques et Universitaires Romandes: Lausanne (in French).
2. Hager, W.H., Oliveto, G. (2002) Shields entrainment condition in bridge hydraulics. *Journal of Hydraulic Engineering* accepted.
3. Hager, W.H., Unger, J., Oliveto, G. (2002) Entrainment criterion for bridge piers and abutments. Intl. Conf. Fluvial Hydraulics *River Flow 2002* Louvain-la-Neuve submitted.
4. Hoffmans, G.J.C.M., Verheij, H.J. (1997) *Scour manual*. Balkema: Rotterdam.
5. Oliveto, G., Hager, W.H. (2002) Temporal evolution of clear-water pier and abutment scour. *Journal of Hydraulic Engineering* tentatively accepted.
6. Raudkivi, A.J. (1998) *Loose boundary hydraulics*. Balkema: Rotterdam.

**NOTATION**

| | |
|---|---|
| $B$ | channel width |
| $D$ | pier diameter |
| $D_*$ | $=(g'/\nu^2)^{1/3}d_{50}$ dimensionless sediment size |
| $d_{50}$ | mean grain size |
| $F_d$ | $=V/(g'd_{50})^{1/2}$ densimetric particle Froude number |
| $F_{di}$ | inception densimetric particle Froude number |
| g | gravitational acceleration |
| g' | $=((\rho_s-\rho)/\rho)g$ reduced gravitational acceleration |
| $h$ | flow depth |
| $R_*$ | $=u_*d_s/\nu$ grain Reynolds number |
| $u_*$ | shear velocity |
| $V$ | cross-sectional velocity |
| $\beta$ | $=b/B$ or $D/B$ contraction ratio |
| $\nu$ | kinematic viscosity |
| $\rho$ | fluid density |
| $\rho_s$ | sediment density |
| $\sigma$ | $=(d_{84}/d_{16})^{1/2}$ sediment non-uniformity |

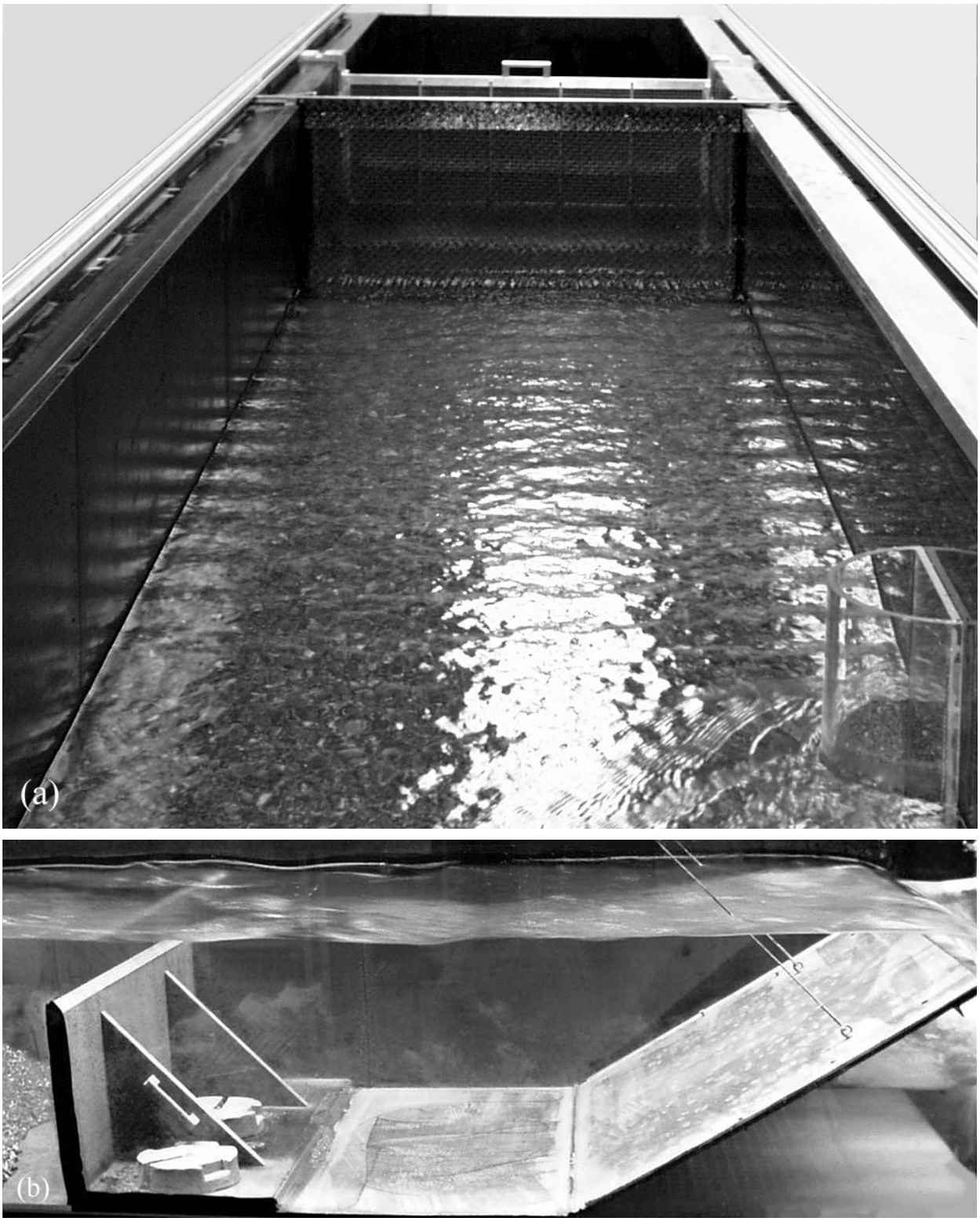


Fig. 1 - VAW scour channel (a) Upstream view with half-cylinder at glass wall, (b) Downstream view with submerged weir and flap gate.

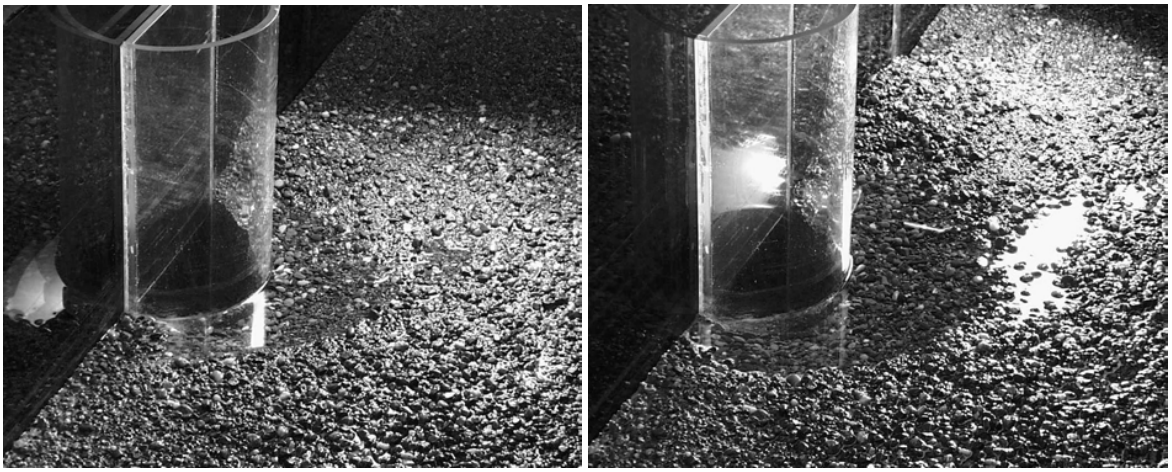

60 s 180 s

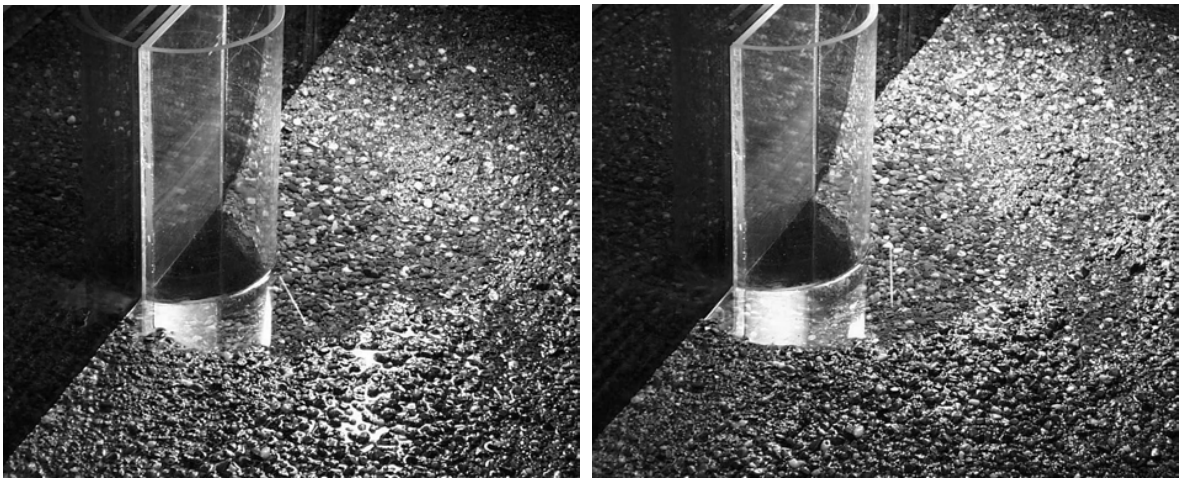

360 s 1200 s

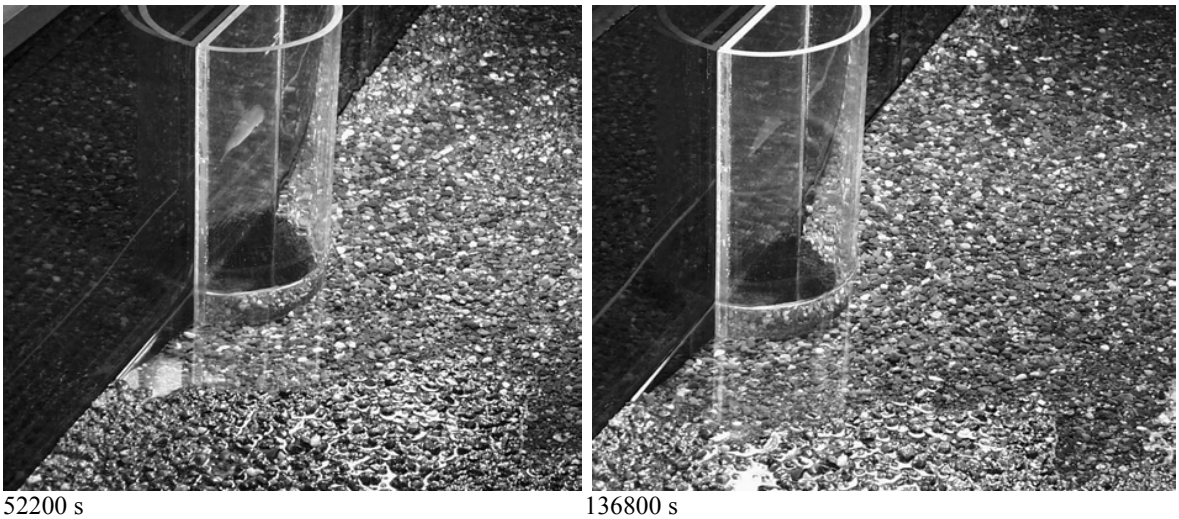

52200 s 136800 s

Fig. 2 - Side view on half-cylinder to visualize scour progress at various times $t$, for $h_o$=0.15 m, $d_{50}$=0.045 m, $\sigma$=2.2 and $F_d$=2.5. Flow direction from bottom to top.

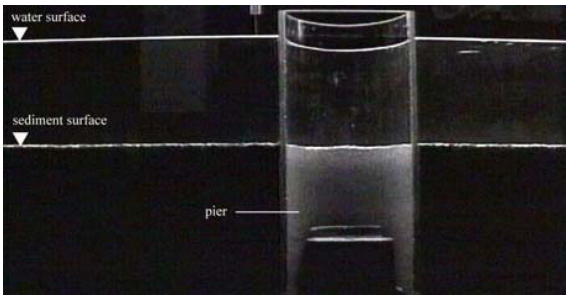

start

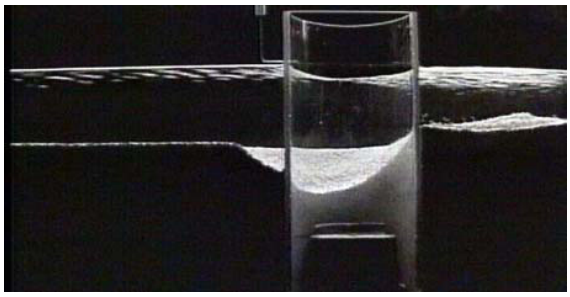
Phase 5

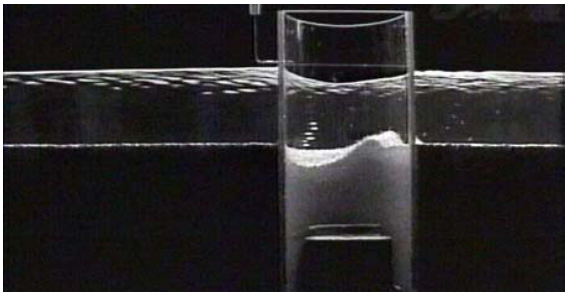
Phase 1

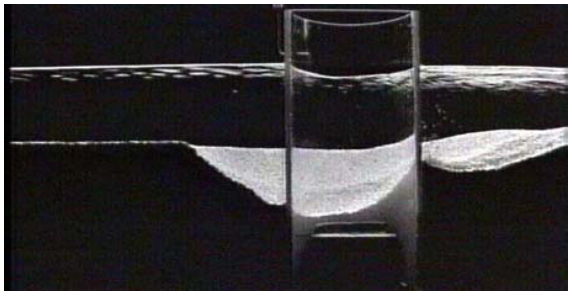
Phase 6

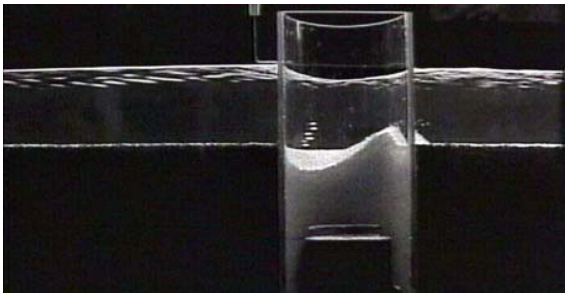
Phase 2

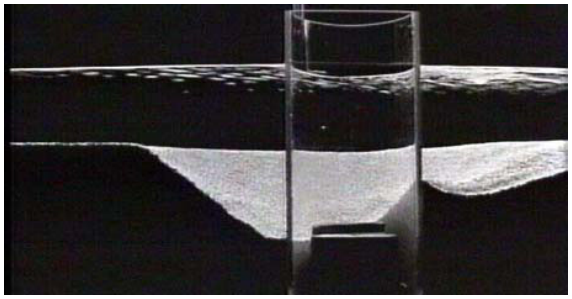
Phase 7

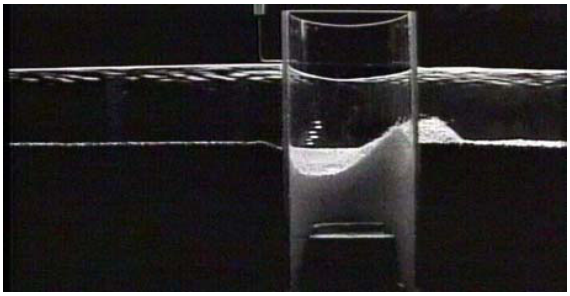
Phase 3

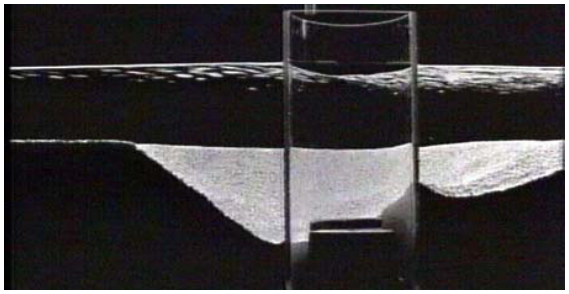
Phase 8

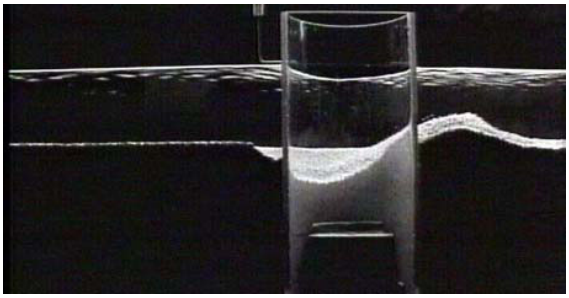
Phase 4

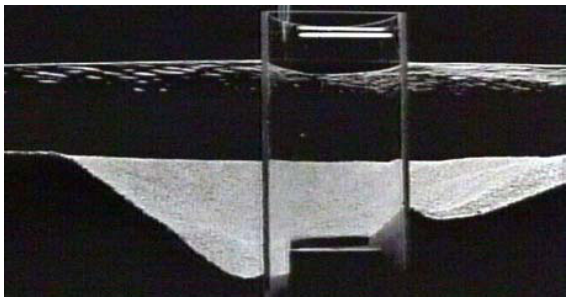
Phase 9

Fig. 3 - Lateral view of scour advance for a half-cylinder with $\rho_s$=1.41 t/m$^3$, $h_o$=0.15 m, $D$=0.257 m, $d_{50}$=0.0033 m and $F_d$=2.50

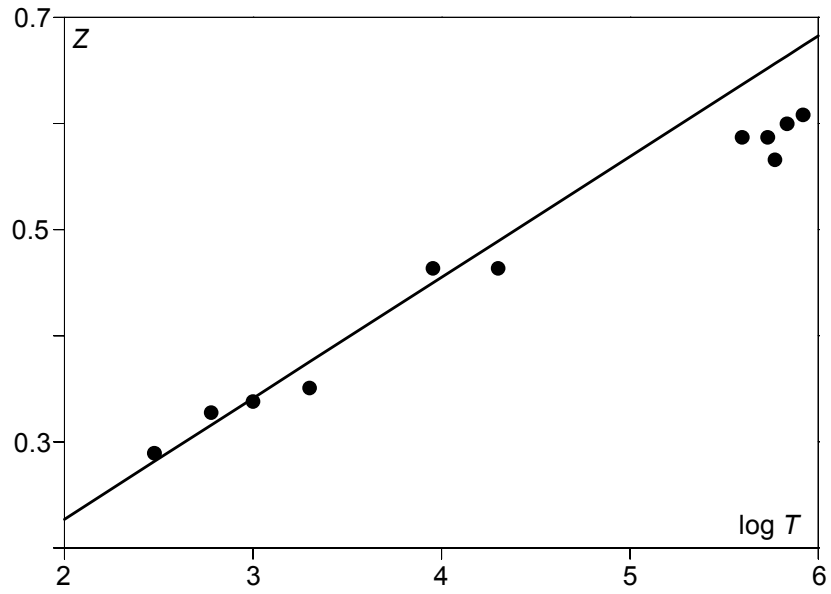


Fig. 4 - Comparison of (●) experimental test data with (—) prediction (5)

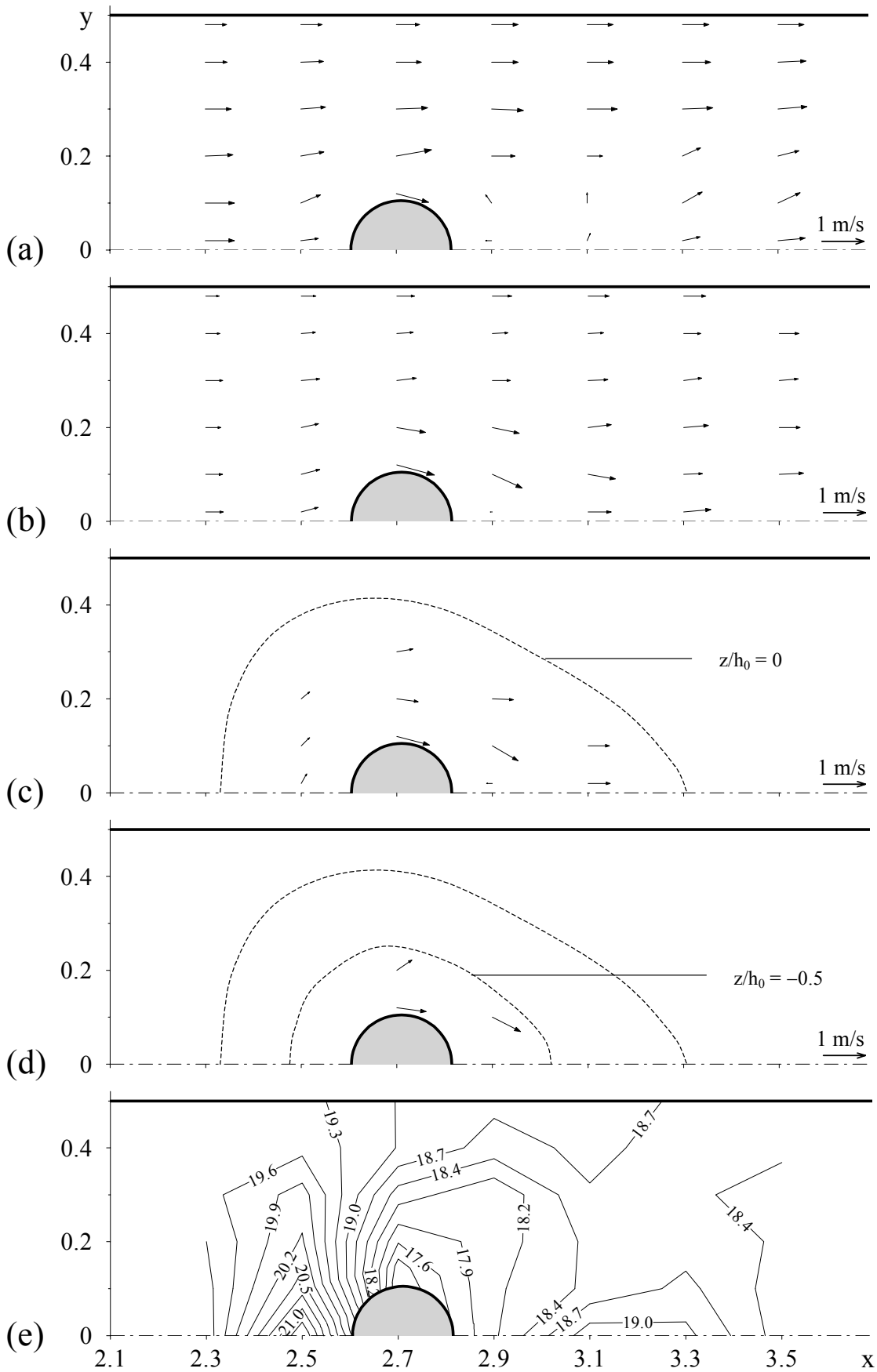


Fig. 5 - Velocity distributions in horizontal layers around a circular pier (a) close to the free surface, (b) at half flow depth, (c) close to sediment bed, (d) half flow depth below sediment bed, and (e) free surface geometry